Why does surface ozone peak in summertime at Waliguan?

Bin Zhu,[1] Hajime Akimoto,[1] Zifa Wang,[2] Kengo Sudo,[1] Jie Tang,[3] and Itsushi Uno[4]

Received 26 May 2004; revised 21 July 2004; accepted 9 August 2004; published 3 September 2004.

[1] The seasonal variation of boundary layer ozone over East Asia is investigated using a regional scale chemical transport model, with the initial and boundary conditions of chemical species obtained from a global chemistry model. Comparisons with observations indicate that the model reproduces the main daily and seasonal features of ozone over eastern Asia. The seasonal variation of ozone has a summer maximum and winter minimum at Waliguan station (on the northeastern edge of the Tibetan Plateau), rather than the spring maximum and summer minimum seen at many other observational sites in the East Asian Pacific rim region. Model results suggest that there is band of a high ozone between 35°N∼45°N from the western boundary (70°E) to 130°E in the summertime. It is concluded that the seasonal transitions associated with the Asian monsoon system and transport from eastern/central China, Central/South Asia and even Europe are significantly responsible for the distinct ozone seasonal cycle at Waliguan. *INDEX TERMS:* 0343 Atmospheric Composition and Structure: Planetary atmospheres (5405, 5407, 5409, 5704, 5705, 5707); 0365 Atmospheric Composition and Structure: Troposphere—composition and chemistry; 0368 Atmospheric Composition and Structure: Troposphere—constituent transport and chemistry. **Citation:** Zhu, B., H. Akimoto, Z. Wang, K. Sudo, J. Tang, and I. Uno (2004), Why does surface ozone peak in summertime at Waliguan?, *Geophys. Res. Lett.*, *31*, L17104, doi:10.1029/2004GL020609.

1. Introduction

[2] The seasonal variation of tropospheric ozone has been documented in many observational studies in the North Hemisphere. These studies indicate that the seasonal cycle of ozone has a spring maximum and summer minimum at many remote surface sites, including East Asia [*Monks*, 2000; *Pochanart et al.*, 2002, and references therein]. *Monks* [2000] suggested that the spring ozone maximum occurs widely across mid-latitudes in the North Hemisphere. In the East Asian Pacific Rim region, most monitoring sites are located downwind of the large anthropogenic emission regions of China, Korea and Japan. The seasonal cycle is attributed to long range transport coupled with continental-oceanic air mass exchange forced by the East Asian monsoon [*Pochanart et al.*, 2002]. The recent work of *Pochanart et al.* [2003] reported an ozone spring maximum-summer minimum at Mondy, a remote site in East Siberia. Modeling studies also reveal such seasonal characteristics of surface ozone in East Asia [*Mauzerall et al.*, 2000]. *Wild and Akimoto* [2001] indicate that intercontinental transport contributes to the regional-scale photochemical production and transport that results in the spring maximum in northeastern Asia.

[3] Waliguan station (36°17′N, 100°54′E) is the highest GAW (Global Atmospheric Watch) station, and is located in a remote region on the northeastern boundary of the Qinghai-Tibetan plateau at a height of 3810 meters. However, measurements at Waliguan station show that ozone has a maximum in summer and a minimum in winter [*Tang et al.*, 1995]. This is distinctly different from other sites in East Asia. The purpose of this study is to explain the surface ozone seasonal characteristics at Waliguan station by using a regional air pollution modeling system (RAPMS).

2. Model Description

[4] The regional air pollution modeling system (RAPMS) is a 3-dimensional regional tropospheric chemical transport model. It consists of two parts, a regional chemical transport model and the Fifth-Generation PSU/NCAR Mesoscale Modeling System, MM5 [*Grell et al.*, 1995], which is used to generate meteorological fields. The initial and boundary conditions for MM5 are obtained from NCAR/NCEP 2.5° × 2.5° reanalysis data sets at 6-hour intervals. The regional chemical transport model was developed by *Wang et al.* [2000], and has been used to simulate atmospheric trace gases and particles, such as SO_x, dust, O_3 and acid rain in East Asia [*Wang et al.*, 2002]. In this version, we implemented the calculation of photolysis rates to use the method of the Models-3 Community Multi-scale Air Quality (CMAQ) modeling system [*Roselle et al.*, 1999]. In this study, the model domain (shown in Figure 1) contains 82 × 64 grid boxes in the east-west and south−north directions with 81 km resolution. This region includes a mixture of urban areas, industrial centers, and rural agricultural areas with both remote continental and oceanic regions, and dramatic variations in topography. In the terrain following height coordinate, the model has 20 σ_z layers unequally spaced from the ground to 15 km, with about 7 layers concentrated in the lowest 1 km of the planetary boundary layer. The chemical transport model includes mass- conserving advection and diffusion processes, parameterization of dry/wet deposition, and the Carbon Bond mechanism IV (CBM-IV) with isoprene chemistry. Anthropogenic emissions of NOx, CO and nonmethane hydrocarbon compounds (NMHC) were obtained from the Emission Database for Global Atmospheric Research (EDGAR) 1° × 1° annual global inventory [*Olivier et al.*, 1996]. NOx emissions from soils and natural hydrocarbon

[1]Frontier Research Center for Global Change, Yokohama, Japan.
[2]Institute of Atmospheric Physics, Chinese Academy of Sciences, Beijing, China.
[3]Chinese Academy of Meteorological Sciences, Beijing, China.
[4]Research Institute for Applied Mechanics of Kyushu University, Kyushu, Japan.

0094-8276/04/2004GL020609$05.00

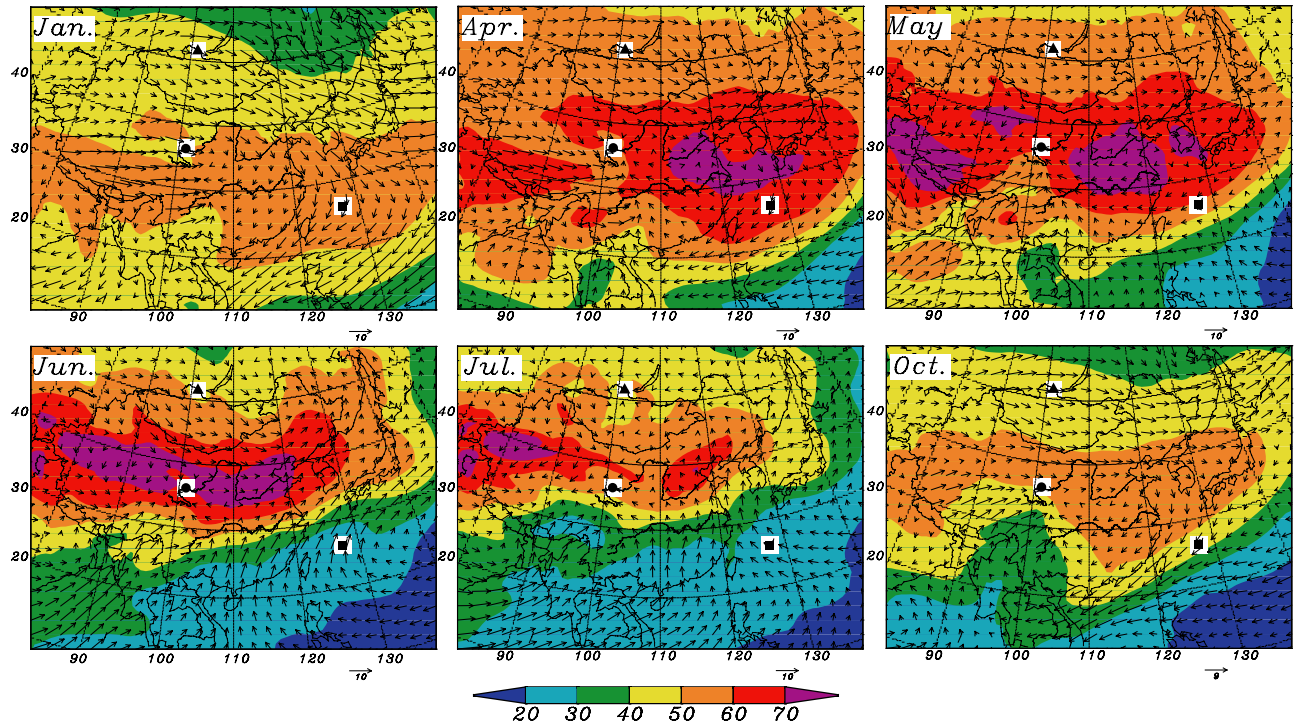

Figure 1. Monthly mean ozone mixing ratios (in ppbv) and wind vector (m/s) in the boundary layer (lowest 1 km) in January, April, May, June, July and October 1996. The locations of Waliguan, Okinawa and Mondy are shown as a black circle, square and triangle, respectively.

emissions were obtained from the Global Emissions Inventory Activity (GEIA) $1° \times 1°$ monthly global inventory [*Benkovitz et al.*, 1996]. The initial and boundary conditions (lateral and top) of long-lived chemical species (O_3, CO, ethane and propane) are taken from the output of a coupled global chemistry-climate model CHASER with roughly 2.8° horizontal resolution. The northern boundary condition of O_3 was modified based on observations, as discussed in the next paragraph. The CHASER model has been described and validated by *Sudo et al.* [2002a, 2002b].

3. Results and Discussion

[5] We evaluate RAPMS by comparing our model results with observations and other modeling studies. Monthly average O_3 mixing ratios and wind fields in the boundary layer simulated by RAPMS for six months in 1996 are shown in Figure 1. The O_3 concentrations and distribution pattern in January correspond well with those of CMAQ simulations for the winter of 1997 [*Zhang et al.*, 2002]. Figure 2 compares hourly-averaged model output with observations at two remote locations in January, April, July and October: one site is at Okinawa (26°50′N, 128°15′E), in the East China Sea and the other at Waliguan. Figure 3 shows the observed and calculated (RAPMS and CHASER) monthly-averaged O_3 variations at Waliguan, Okinawa and Mondy (51°39′N, 100°55′E) in East Asia. In general, our regional model reproduces well the daily and seasonal variations of O_3 caused by large scale atmospheric transport and photochemical reactions. Although the global model (CHASER) approximately reproduces the O_3 seasonal features, it cannot capture the daily and seasonal variation of O_3 as well because of its coarse resolution. For example, at Mondy CHASER overestimates O_3 in the summer and underestimates O_3 during the rest of the year, and it overestimates O_3 in May at Waliguan. For this reason, for the regional model runs, we decreased the northern boundary O_3 value by 8ppbv from CHASER in July and August and increased it by 6ppbv from January to April and October to December.

[6] From Figures 1 and 3, we can see that there are distinct seasonal distribution features of O_3 over East Asia. The monthly mean wind flow patterns shown in Figure 1 highlight the typical pollutant transport pathways in different months. In most rural and remote East Asian Pacific rim

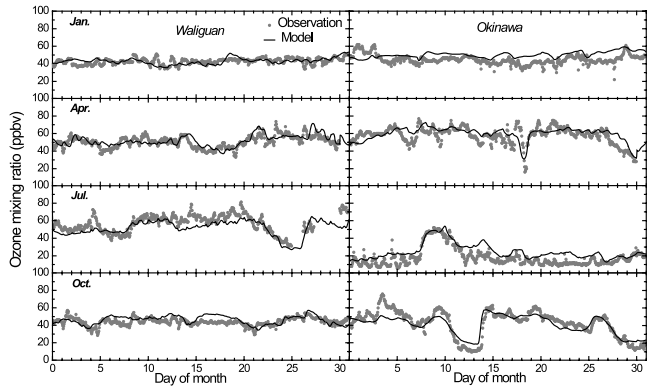

Figure 2. Comparisons between the hourly-averaged ozone (solid line) simulated by RAPMS for the lowest model layer and observed hourly ozone (grey dot) at Waliguan and Okinawa in January, April, July and October 1996.

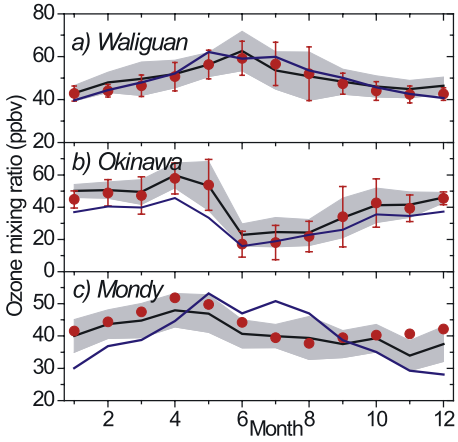

Figure 3. Monthly-averaged surface ozone variations at Waliguan, Okinawa and Mondy. All observed (red dots) and simulated (black: regional model, blue: global model) data are for 1996, except observations at Mondy which are an average of 1997 and 1998 data. Vertical bars on the observational data indicate one standard deviation of the hourly means. Grey areas indicate one standard deviation of the regional model results.

regions (such as Okinawa), O_3 has a spring maximum and summer minimum. High O_3 in spring comes from continental outflow and active photochemistry, and low O_3 in summer from the Pacific ocean where background concentrations are low. At Mondy, located at high latitude in central Asia, the spring maximum-summer minimum largely reflects the seasonal impacts of transport from distant upwind some regions [*Pochanart et al.*, 2003; *Wild and Akimoto*, 2001].

[7] In contrast with other observational sites, Figures 1 and 3a show a different seasonal cycle at Waliguan station. The O_3 has a summer maximum and winter minimum.

[8] In Figure 1, we see clearly a northward shift in peak O_3 over East Asia from winter to summer. From winter to spring, O_3 levels increase throughout East Asia because of enhanced photochemical production and outflow from the continent. From April, the southern edge of the band of high O_3 shifts northward. In April, the southern edge defined by 60ppbv is at about 22°N, in May at 25°N, in June at 32°N, and it reaches its northmost position at 36°N in July 1996. It is interesting to see that from spring to summer, the area of high O_3 (>60 ppbv) shrinks into a narrow band between 35°N∼45°N over 70°E∼125°E (see Figure 1). South Asia and East Asia are the prominent monsoon regions in the world. In East Asia, the summer flow pattern is controlled by the Indian tropical monsoon and East Asian sub-tropic monsoon systems. In the lower troposphere, the southern monsoon flow can sometimes reach as far as 40°N, and brings marine air masses with low background O_3 to the north. Most of the monitoring sites in the East Asian Pacific rim region are influenced by marine air masses in summer; this explains the O_3 minimum in the summer in the continental rim region in Asia. From September, with the weakening of the southerly wind and the appearance of high pressure over Mongolia and Siberia, the band of high O_3 is pushed southwards and the O_3 concentration decreases over almost all area north of 35°N (Figure 1, Oct.). A similar seasonal cycle of O_3 is seen in global modeling studies [*Sudo et al.*, 2002b; *Lelieveld and Dentener*, 2000].

[9] Figures 4a and 4b show the monthly mean net transport flux and net O_3 photochemical production (ppbv/day) in the boundary layer in July 1996, respectively. Figure 4a shows a band with a high import flux over west of 110°E, corresponding well with the band of high O_3. Figure 4b illustrates the strong net photochemical O_3 production in summer over the polluted regions in East Asia, including Eastern China, Korea and Japan. Although photochemical O_3 production is not weak over polluted regions south of 30°N in the summertime, O_3 cannot accumulate because of export by the strong southerly flow. The budget of O_3 in the boundary below 1 km in an area 164,025 km^2 around Waliguan, Mondy and Okinawa are shown in Table 1. Negative values indicate mass fluxes out of the sample column. The table shows that the O_3 sources are mainly controlled by horizontal transport at Waliguan. In summer, vertical transport only contributes a small part to the net transport. The CHASER model indicates that O_3 exchange from the stratosphere to the troposphere is minimum in summer. The net O_3 photochemical production is small and negative at Waliguan, in agreement with the estimate by *Ma et al.* [2002]. Although Mondy is at almost the same longitude as Waliguan, it is 15° further north and hence experiences lower horizontal transport fluxes than Waliguan. This is the main reason for the different O_3 seasonal cycles at these two sites. In Table 1, we see that the transport fluxes are higher at Mondy and Okinawa in spring than in other seasons.

[10] We conclude that to the west of 110°E, there is a mid-latitude band of high O_3 in summer over East Asia which is maintained by transport. In polluted regions east of 110°E, however, the O_3 concentration is controlled by

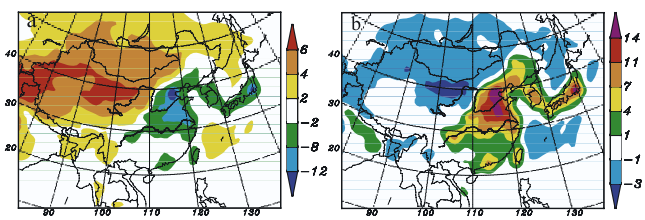

Figure 4. Monthly-averaged net transport flux (a) and net ozone production (b) in the boundary layer in July. Units are ppb/day.

Table 1. Sources and Sinks of O_3 in the Boundary Layer in 1996[a]

		HT	VT	Net	Chem.	Dry Dep.
WLG	Jan.	13.2	−7.8	5.4	1.2	−6.8
	Apr.	16.1	−10.1	6.0	1.1	−7.4
	Jun.	10.3	1.3	11.6	−2.2	−9.2
MD	Jan.	3.8	2.9	6.7	−0.2	−6.7
	Apr.	10.7	−3.0	7.7	−0.1	−7.6
	Jun.	6.4	0.9	7.3	−0.8	−6.6
ON	Jan.	6.7	−1.6	5.1	−1.3	−3.9
	Apr.	4.9	1.7	6.6	−1.8	−4.5
	Jun.	−0.7	3.3	2.6	−1.1	−1.9

[a]Units are 10^8 mole/month. HT represents the contributions from horizontal transport and diffusion, VT the contributions from vertical transport and diffusion; and WLG, MD, ON denote Waliguan, Mondy and Okinawa, respectively.

photochemical production. Normally high levels of O_3 are transported from the western boundary north of 35°N because of blocking by the Himalayas and the Tibetan plateau south of 35°N. Many opportunities, high levels of photochemically produced O_3 are transported from central and eastern China. *Wild and Akimoto* [2001] suggested that intercontinental transport from Europe can raise East Asian O_3 levels although not by a very large amount in summer. CHASER model simulations [*Sudo et al.*, 2002b] show high O_3 levels moving from South Asia (in April) to Central Asia (in July) because of the effect of the Indian summer monsoon. As a result, the transport of high O_3 air masses from eastern/central China, Central/South Asia and even Europe contributes significantly to the band of high O_3 in Western China in the summertime.

4. Summary

[11] We have investigated the seasonal variation of boundary layer ozone over East Asia using the regional scale air pollution modeling system (RAPMS). RAPMS is able to reproduce the observed features of surface O_3 over East Asia and its daily and seasonal variations. The seasonal distribution of O_3 is mainly controlled by the evolution of the East Asian monsoon system in combination with photochemical production. In our simulations, we find that there is a band of high O_3 between 35°N∼45°N from 70°E (the western boundary of the model) to 130°E in the summertime. In polluted regions to the east of 110°E, the high O_3 levels are mainly controlled by photochemical production and result in regional O_3 export. But to the west of 110°E, the band of high O_3 is caused by transport, and shows weak photochemical destruction. This O_3 maybe transported from eastern/central China, Central/South Asia and even Europe. The results give a reasonable explanation for the distinct seasonal variations of surface O_3 (summer maximum and winter minimum) seen at Waliguan station (on the northeastern edge of the Tibetan plateau).

[12] **Acknowledgments.** We thank Dr. P. Pochanart of the Frontier Research Center for Global Change (FRCGC) for providing ozone measurement data. We acknowledge two anonymous reviewers for useful comments on the manuscript. Dr. Oliver Wild and Dr. Donald D. Lucas of the FRCGC is gratefully acknowledged for suggestions on improving the manuscript.

References

Benkovitz, C. M., M. T. Schultz, J. Pacyna et al. (1996), Global gridded inventories of anthropogenic emissions of sulfur and nitrogen, *J. Geophys. Res.*, *101*, 29,239–29,253.

Grell, G. A., J. Dudhia, and D. R. Stauffer (1995), A description of the Fifth-Generation Penn State/NCAR Mesoscale Model (MM5), *Tech. Note NCAR/TN-398+STR*, 122 pp., Natl. Cent. for Atmos. Res., Boulder, Colo.

Lelieveld, J., and F. Dentener (2000), What controls tropospheric ozone?, *J. Geophys. Res.*, *105*, 3531–3551.

Ma, J., J. Tang, X. J. Zhou, and X. S. Zhang (2002), Estimates of the chemical budget for ozone at Waliguan Observatory, *J. Atmos. Chem.*, *41*, 21–48.

Mauzerall, D. L., D. Narita, H. Akimoto et al. (2000), Seasonal characteristics of tropospheric ozone production and mixing ratios over East Asia: A global three-dimensional chemical transport model analysis, *J. Geophys. Res.*, *105*, 17,895–17,910.

Monks, P. S. (2000), A review of the observations and origins of the spring ozone maximum, *Atmos. Environ.*, *34*, 3545–3561.

Olivier, J. G. J., et al. (1996), Description of EDGAR version 2.0, *Rep. 771060 002/TNO-MEP*, *Rep. R96/119*, Natl. Inst. of Public Health and the Environ., Amsterdam.

Pochanart, P., H. Akimoto, Y. Kinjo, and H. Tanimoto (2002), Surface ozone at four remote island sites and the preliminary assessment of the exceedances of its critical level in Japan, *Atmos. Environ.*, *36*, 4235–4250.

Pochanart, P., H. Akimoto, Y. Kajii et al. (2003), Regional background ozone and carbon monoxide variations in remote Siberia/East Asia, *J. Geophys. Res.*, *108*(D1), 4028, doi:10.1029/2001JD001412.

Roselle, S. J., K. L. Schere, and J. E. Pleim (1999), Photolysis rates for CMAQ, in *Science Algorithms of the EPA Models-3 Community Multiscale Air Quality (CMAQ) Modeling System*, edited by D. W. Byun and J. K. S. Ching, *Rep. EPA 600/R-99/030*, chap. 14, U.S. Environ. Protect. Agency Atmos. Model. Div., Research Triangle Park, N. C.

Sudo, K., M. Takahashi, J. Kurokawa, and H. Akimoto (2002a), CHASER: A global chemical model of the troposphere: 1. Model description, *J. Geophys. Res.*, *107*(D17), 4339, doi:10.1029/2001JD001113.

Sudo, K., M. Takahashi, and H. Akimoto (2002b), CHASER: A global chemical model of the troposphere: 2. Model results and evaluation, *J. Geophys. Res.*, *107*(D21), 4586, doi:10.1029/2001JD001114.

Tang, J., C. Luo, G. Ding et al. (1995), Surface ozone measurement at China GAW baseline observatory, paper presented at the Conference on the Measurement and Assessment of Atmospheric Composition Change, World Meteorol. Organ., Int. Global Atmos. Chem., Beijing.

Wang, Z., W. Sha, and H. Ueda (2000), Numerical modeling of pollutant transport and chemistry during a high-ozone event in northern Taiwan, *Tellus, Ser. B*, *52*, 1189–1205.

Wang, Z., H. Akimoto, and I. Uno (2002), Neutralization of soil aerosol and its impact on the distribution of acid rain over East Asia: Observations and model results, *J. Geophys. Res.*, *107*(D19), 4389, doi:10.1029/2001JD001040.

Wild, O., and H. Akimoto (2001), Intercontinental transport of ozone and its precursors in a three-dimensional global CTM, *J. Geophys. Res.*, *106*, 27,729–27,744.

Zhang, M., I. Uno, S. Sugata et al. (2002), Numerical study of boundary layer ozone transport and photochemical production in east Asia in the wintertime, *Geophys. Res. Lett.*, *29*(11), 1545, doi:10.1029/2001GL014368.

H. Akimoto, K. Sudo, and B. Zhu, Frontier Research Center for Global Change, Yokohama, Kanagawa 236-0001, Japan. (akimoto@jamstec.go.jp; kengo@jamstec.go.jp; binzhu@jamstec.go.jp)

J. Tang, Chinese Academy of Meteorological Sciences, Beijing 100081, China. (tangj@cams.cma.gov.cn)

I. Uno, Research Institute for Applied Mechanics of Kyushu University, Kasuga Park 6-1, Kasuga 816-8580, Japan. (iuno@riam.kyushu-u.ac.jp)

Z. Wang, LAPC/NZC, Institute of Atmospheric Physics, Chinese Academy of Sciences, Beijing 100029, China. (zifawang@mail.iap.ac.cn)